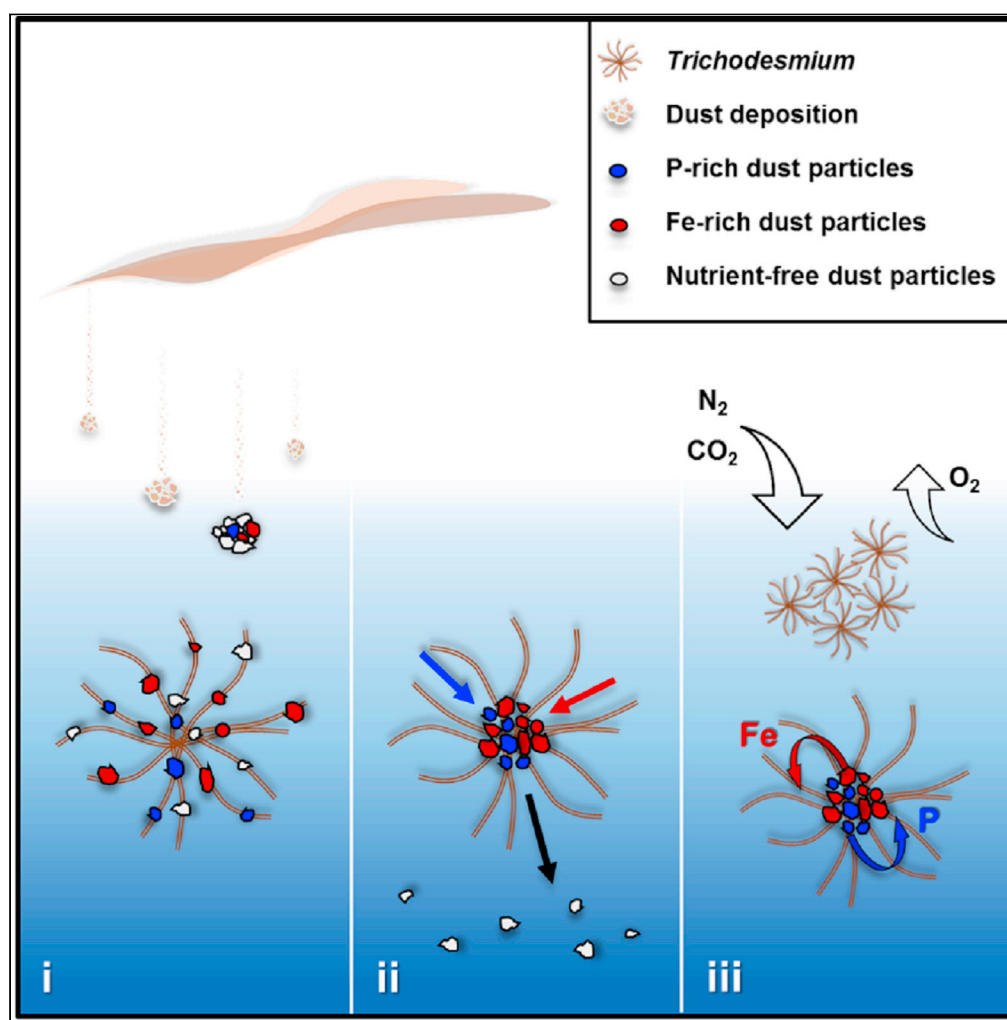


## Article

Colonies of the marine cyanobacterium *Trichodesmium* optimize dust utilization by selective collection and retention of nutrient-rich particles

Siyuan Wang,  
Coco Koedooder,  
Futing Zhang, Nivi  
Kessler, Meri  
Eichner, Dalin Shi,  
Yeala Shaked

yeala.shaked@mail.huji.ac.il

**Highlights**

Natural *Trichodesmium* colonies collect and maintain dust within their colony core

Using synthetic particles we tested if colonies select the particles they collect

Colonies selectively collect and retain nutrient-rich over nutrient-free particles

Selective collection of particles optimizes their nutrient acquisition from dust

Wang et al., iScience 25,  
103587  
January 21, 2022 © 2021 The  
Authors.  
[https://doi.org/10.1016/  
j.isci.2021.103587](https://doi.org/10.1016/j.isci.2021.103587)

## Article

Colonies of the marine cyanobacterium *Trichodesmium* optimize dust utilization by selective collection and retention of nutrient-rich particlesSiyuan Wang,<sup>1,2</sup> Coco Koedooder,<sup>1,2,3</sup> Futing Zhang,<sup>1,2,4</sup> Nivi Kessler,<sup>1,6</sup> Meri Eichner,<sup>5</sup> Dalin Shi,<sup>4</sup> and Yeala Shaked<sup>1,2,7,\*</sup>

## SUMMARY

***Trichodesmium*, a globally important, N<sub>2</sub>-fixing, and colony-forming cyanobacterium, employs multiple pathways for acquiring nutrients from air-borne dust, including active dust collection. Once concentrated within the colony core, dust can supply *Trichodesmium* with nutrients. Recently, we reported a selectivity in particle collection enabling *Trichodesmium* to center iron-rich minerals and optimize its nutrient utilization. In this follow-up study we examined if colonies select Phosphorus (P) minerals. We incubated 1,200 *Trichodesmium* colonies from the Red Sea with P-free CaCO<sub>3</sub>, P-coated CaCO<sub>3</sub>, and dust, over an entire bloom season. These colonies preferably interacted, centered, and retained P-coated CaCO<sub>3</sub> compared with P-free CaCO<sub>3</sub>. In both studies, *Trichodesmium* clearly favored dust over all other particles tested, whereas nutrient-free particles were barely collected or retained, indicating that the colonies sense the particle composition and preferably collect nutrient-rich particles. This unique ability contributes to *Trichodesmium*'s current ecological success and may assist it to flourish in future warmer oceans.**

## INTRODUCTION

Phosphorus (P) is commonly regarded as the ultimate limiting nutrient for phytoplankton growth and plays a central biogeochemical role in marine environments (Karl, 2000, 2014; Martiny et al., 2019). On a global scale, although Nitrogen (N) deficits may be offset by N<sub>2</sub> fixation, changes in P supply to the ocean surface can exert a strong control on future ocean productivity and downward carbon export (Bopp et al., 2013; Moore et al., 2008; Tyrrell, 1999; Wu et al., 2000). P has also been identified as the limiting nutrient in regions such as the western North Atlantic Ocean (Ammerman et al., 2003; Mather et al., 2008) and the eastern Mediterranean Sea (Thingstad et al., 2005) and as such regulate phytoplankton growth, abundance, and diversity (Chien et al., 2016; Mills et al., 2004).

Desert dust is considered an important nutrient source to stratified ocean gyres and remote open ocean areas (Jickells et al., 2005). Most research centers on iron (Fe) inputs from Fe-rich dust (Johnson et al., 2010; Mahowald et al., 2005; Mélançon et al., 2016; Sarthou et al., 2003; Shoenfelt et al., 2018), due to the large extent of Fe-limitation in the ocean. Yet, dust and other aerosols also contain 0.1%–10% P (Anderson et al., 2010; Stockdale et al., 2016), with estimated deposition to the ocean of 0.8–1.4 Tg (10<sup>12</sup> g) P yr<sup>-1</sup> (Mahowald et al., 2008; Wang et al., 2015). Phosphorus in dust is predominantly present as apatite, an inorganic mineral-P form, which is almost insoluble in seawater. Other, less abundant but more bioavailable P-forms include metal-bound P (e.g., Al-P and Fe-P), absorbed P, and organic P (Stockdale et al., 2016; Zhang et al., 2018). Upon deposition of dust on the ocean surface, only a fraction of surface-bound P is dissolved and made available for biological utilization prior to sedimentation (~10% solubility, yielding 0.24 Tg dissolved P yr<sup>-1</sup>) (Mahowald et al., 2008). Despite its low solubility, P deposition from dust was shown to impact ecosystems in some open ocean and coastal areas, as well as terrestrial environments such as lakes and forests (Barkley et al., 2019; Gross et al., 2020; Herut et al., 2016; Markaki et al., 2010; Okin et al., 2004; Pulido-Villena et al., 2010).

An organism that is consistently reported to flourish and increase its N<sub>2</sub> fixation rates following dust addition is *Trichodesmium* spp. (Chen et al., 2011; Fernández et al., 2010; Lenés et al., 2008). This cyanobacterium is prevalent throughout the tropical and subtropical ocean, where it often forms enormous surface

<sup>1</sup>The Freddy and Nadine Herrmann Institute of Earth Sciences, Edmond J. Safra Campus, Givat Ram, Hebrew University of Jerusalem, Jerusalem, Israel

<sup>2</sup>The Interuniversity Institute for Marine Sciences in Eilat, Eilat, Israel

<sup>3</sup>Israel Limnology and Oceanography Research, Haifa, Israel

<sup>4</sup>State Key Laboratory of Marine Environmental Science, Xiamen University, Xiamen, Fujian, People's Republic of China

<sup>5</sup>Laboratory of Photosynthesis, Center Algatech, Institute of Microbiology of the Czech Academy of Sciences, Třeboň, Czech Republic

<sup>6</sup>Present address: The water authority, 7 Bank of Israel st, Jerusalem, Israel

<sup>7</sup>Lead contact

\*Correspondence: yeala.shaked@mail.huji.ac.il  
<https://doi.org/10.1016/j.isci.2021.103587>



accumulations (“blooms”) visible to the naked eye and from space (Bergman et al., 2013). *Trichodesmium* blooms are often associated with dust deposition, specifically in the tropical Atlantic, downwind from the Saharan desert dust plume (Bif and Yunes, 2017; Ramos et al., 2005; Rivero-Calle et al., 2016). *Trichodesmium* blooms comprise individual filaments as well as colonies in fusiform (tuft) and radial (puff) shapes, composed of tens to hundreds of individual filaments (Bergman et al., 2013; Berman-Frank et al., 2001; Capone et al., 1997; Dyrhman et al., 2002). *Trichodesmium* is a successful bloom-forming nitrogen fixer from oligotrophic tropical and subtropical oceans, generating 60 to 80 Tg of new N annually, almost 40% of annual global nitrogen fixation (Capone and Carpenter, 1982). *Trichodesmium* contributes to sustaining marine life via the active release and release upon death and decay of key nutrients such as carbon and nitrogen, hence making it a vital player in the biogeochemical cycling of basic elements in contemporary and past oceans (Deutsch et al., 2007).

In nutrient-poor oligotrophic oceans, *Trichodesmium*, which is capable of supplying its N requirements by fixing atmospheric N<sub>2</sub>, often becomes limited or co-limited by Fe and P (Held et al., 2020b; Mills et al., 2004; Wu et al., 2000). Some reports suggest that *Trichodesmium* is primarily P-stressed in the North Atlantic, and primarily Fe-stressed in the Pacific, owing to the relative Fe and P availability in these regions (Chappell et al., 2012; Frischkorn et al., 2018; Hynes et al., 2009; Orchard et al., 2010a; Sañudo-Wilhelmy et al., 2001; Sohm et al., 2008; Tang et al., 2020). *Trichodesmium* is uniquely adapted to chronic P limitation, with an array of recently discovered pathways including hydroxylation of organic ester-bound phosphate (Orchard et al., 2009), C-P bond lyase of phosphonates (Dyrhman et al., 2006), utilization of phosphite (Polyviou et al., 2015), substitution of phospholipids with sulfolipids (Van Mooy et al., 2009), and P storage as polyphosphate (Orchard et al., 2010b). The low surface area to volume ratio of large *Trichodesmium* colonies imposes a strong limitation on the acquisition of dissolved nutrients (Sunda and Huntsman, 1995).

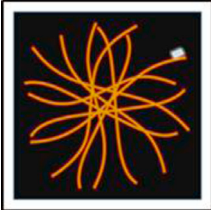








On the other hand, *Trichodesmium* colonies are uniquely adapted to utilize air-borne dust deposited on the ocean surface as a source of nutrients (Langlois et al., 2012; Moore et al., 2009; Rubin et al., 2011; Rueter et al., 1992). Large colonies are more likely to encounter dust particles compared with single cells or filaments as their intricate morphology ensures the effective capture and retention of particles (Bif and Yunes, 2017). Previous studies documented that colonies further improve dust retention by active particle shuttling from the periphery to the colony core in a coordinated movement by trichomes (Rubin et al., 2011; Rueter et al., 1992). Moreover, Kessler et al. (2020a) reported that *Trichodesmium* has the ability to select the particles they center based on their nutritional value (Kessler et al., 2020a). A strong preference for Fe-rich particles over Fe-free particles was observed by incubating Red Sea natural colonies with dust, Fe-free and Fe-coated silica minerals (Kessler et al., 2020a). In addition, the selective removal of Fe-free particles further indicated that colonies can chemically sense Fe on particles and optimize the supply of Fe from dust (Kessler et al., 2020a).

Kessler et al. (2020a) observed a strong preference for dust over Fe-coated minerals, suggesting that the colonies may seek additional nutrients from dust (Kessler et al., 2020a). In the oligotrophic Gulf of Aqaba, *Trichodesmium* is often subjected to P limitation, as documented by high alkaline phosphatase activity, an enzyme indicative of P stress (Mackey et al., 2007; Stihl et al., 2001). Given the low dissolved P concentrations (Fuller et al., 2005; Kuhn et al., 2018) and the high dust deposition in the Gulf (Chen et al., 2007; Torfstein et al., 2017), we hypothesize that *Trichodesmium* can utilize dust as a source of P, possibly assisted by the selective collection of P-rich particles.

Here, we follow up on our previous findings of particle selection by *Trichodesmium* and explore the ability of natural colonies to differentiate between P-free and P-rich particles. We conducted detailed microscopic observations on ~1,200 natural colonies from the Gulf of Aqaba incubated with high-purity CaCO<sub>3</sub> (herein referred to as P-free CaCO<sub>3</sub>) or P-adsorbed CaCO<sub>3</sub> (herein referred to as P-rich CaCO<sub>3</sub>) synthesized to mimic the readily dissolved surface-adsorbed P in dust. We repeated these 24-h incubations during 17 individual days throughout an entire bloom season, testing in parallel the collection and retention of dust. As in Kessler et al. (2020a), we assigned scores for three individual interaction parameters. In addition, we combined them to generate an index describing colony-particle interaction over time. In parallel, we tested whether natural colonies are P-limited, using qPCR expression of the high-affinity phosphate-binding protein *sphX*.

## RESULTS

In our study we characterized colony-particle interactions by assigning three discrete interaction parameters (Figure 1) combining them to an index describing the colony-particle interaction over time (Figure 2).

Parameter and description	Scores		
<p><b>Short-term (ST) interaction</b></p> <p>Time: 15 min</p> <p>Scores were determined by the number of particles associated with the colony at 15 min after particle addition.</p>	 <p>None (-) = &lt;3</p>	 <p>Mild (+) = 3-10</p>	 <p>Strong (++) = &gt;10</p>
<p><b>Particle transfer from periphery to center (Centering)</b></p> <p>Time: 1.5 h</p> <p>Scores were determined by both the number of particles identified and their locations on the colony after 1.5 h.</p>	 <p>No particles (NP) = no particles on the colony</p>	 <p>No centering (O) = few particles on periphery; none in the center</p>	 <p>Strong centering (*) = many particles in the colony center</p>
<p><b>Long-term (LT) interaction</b></p> <p>Time: Overnight (13-27 h)</p> <p>Scores were determined by the number of particles remaining on the colony after overnight-incubation.</p>	 <p>None (-) = &lt;3</p>	 <p>Mild (+) = 3-10</p>	 <p>Strong (++) = &gt;10</p>

**Figure 1. Characterization scheme of colony-particle interactions**

Characterization of colony-particle interactions during three time points, representing three different parameters. A score and color-code was assigned for each parameter according to the criteria shown, following the criteria of Kessler et al. (2020a) with some modifications. Scores were assigned to alive and integral colonies.

We refer to the following two terms: (1) interaction strength, the tendency of colonies to interact with particles, and (2) selectivity, the preference of colonies for P-rich over P-free  $\text{CaCO}_3$ .

### Selective collection of P-rich particles—single day data

We first present a single sampling day (October 28, 2019) where we obtained 80 freshly collected Red Sea colonies, showing a statistically significant preference for P-rich over P-free particles in all interaction parameters (Figures 3A–3C;  $p < 0.05$ , Table S4). On that day, the initial interactions (ST) were mostly positive (+/++), with 80% of the colonies interacting with both P-rich and P-free  $\text{CaCO}_3$  particles (Figure 3A). The percentage of colonies collecting many particles (++) was much higher for P-rich  $\text{CaCO}_3$  (60%) than for P-free  $\text{CaCO}_3$  (20%, Figure 3A). The selectivity was even more evident when looking at the parameter of

Categories	Pattern	Parameter-Score		
		ST	Centering	LT
Inactive	A	-	NP	-
	D	-	O	-
Slightly active	J	+	NP	-
	M	+	O	-
	N	+	O	+
Active	P	+	*	-
	Q	+	*	+
	V	++	O	-
	W	++	O	+
	Y	++	*	-
Very active	Z	++	*	+
	Za	++	*	++

**Figure 2. Single colony index**

The integration of all three scored interaction parameters assigned to each colony (Figure 1) into a single value describing the colony-particle interaction over time. From all 27 possible combinations of the three interaction parameters, 12 common patterns were found to represent ~90% of the colonies during the incubation experiments. These 12 patterns are further grouped into four categories ranked and color-coded according to the strength of colony-particle interactions.

centering, which was examined 1.5 h after particle addition (Figures 1 and 3B). A strong centering score (colored purple; \*), marking the active translocation of particles to the colony core, was assigned to 90% of colonies subjected to P-rich CaCO<sub>3</sub>, whereas only 20% of the colonies centered P-free CaCO<sub>3</sub> (Figure 3B). In fact, almost half of the colonies that initially (ST) interacted with P-free CaCO<sub>3</sub> were particle-free at this stage (NP), indicating that they removed P-free CaCO<sub>3</sub> shortly after particle additions. This trend of particle removal continued during the overnight incubations, as is evident by the “lighter” bars in Figure 3C compared with Figure 3A. Furthermore, the removal of particles was highly selective, with 80% of the colonies incubated with P-free CaCO<sub>3</sub> not retaining any particles toward the end of the incubation (Figure 3C). Combined, all interaction parameters indicated that, on October 28, 2019, natural *Trichodesmium* colonies from the Red Sea were able to detect particle-P and modify their behavior to favor the collection and retention of P-rich over P-free particles.

### Selective collection of P-rich particles—entire season

We repeated these experiments during 17 different days, and when combined, we observed a statistically significant selectivity in all interaction parameters (Figure 4A;  $p < 0.05$ , Table S4). Throughout the season, the interaction strength was higher for initial interactions (ST) compared with overnight interactions (LT), indicating that colonies removed some of the particles they had initially collected (Figure 4A). The removal of particles was more pronounced for P-free than P-rich CaCO<sub>3</sub>, further indicating that natural *Trichodesmium* colonies can distinguish among these minerals.

In order to integrate the interaction scores into a single parameter and follow the behavior of individual colonies throughout the incubation time frame, we re-analyzed our data according to the single colony index. Briefly, this index describes the tendency of a single colony to collect, center, and retain particles (see STAR Methods). Our dataset yielded 12 common patterns, which we subsequently grouped into four categories termed “inactive,” “slightly active,” “active,” and “very active” (Figure 2).

As with the discrete interaction parameters, this combined index reveals clear differences between P-free and P-rich particles. A higher proportion (50%) of the colonies incubated with P-rich CaCO<sub>3</sub> grouped into the

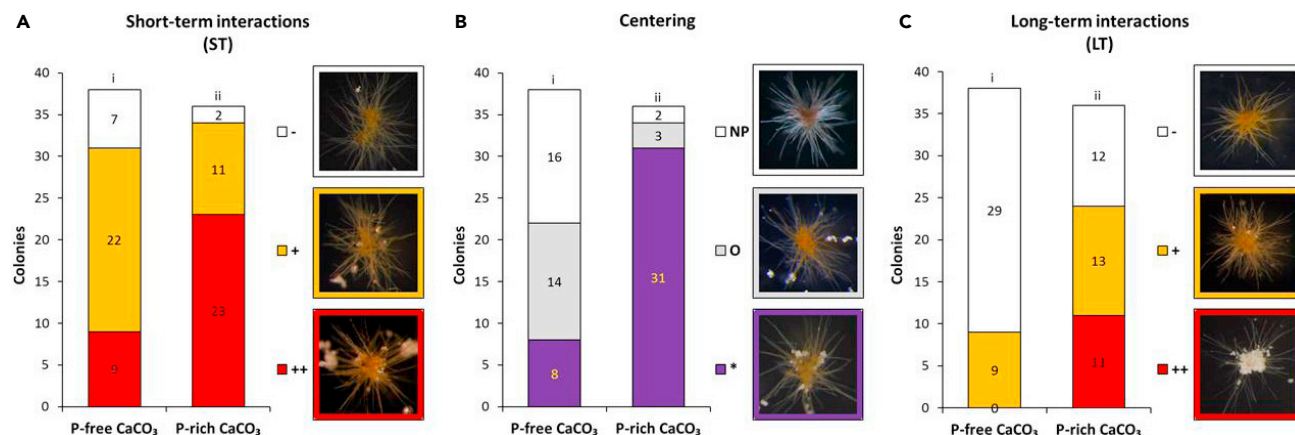


**Figure 3. Interactions between natural *Trichodesmium* colonies and P-free or P-rich CaCO<sub>3</sub> in an experiment conducted on October 28, 2019** (A) Short-term (ST) interactions, (B) Centering, and (C) Long-term (LT) interactions (see Figure 1). Pictures of colonies with particles representing each parameter score are shown next to each panel. Statistically significant differences between particle types ( $p < 0.05$ ) were found for all parameters, as labeled by letters. Natural colonies preferably interacted, centered, and retained P-rich particles in comparison with P-free particles.

“active” and “very active” categories (Figure 4B). In contrast, a higher proportion (50%) of colonies incubated with P-free CaCO<sub>3</sub> were placed in the inactive and slightly active categories (Figure 4B). Thus, our findings were able to further demonstrate that *Trichodesmium* selectively collects P-rich over P-free particles.

#### Day-to-day and seasonal variations in colony-particle interactions

We observed day-to-day and seasonal variations in both interaction strength and selectivity (Figure 5). For example, colonies were highly interactive on November 19 but mostly inactive on October 22 (Figure 5). Colonies were highly selective on October 28 but mostly nonselective on October 27 (Figure 5). In addition, the interaction strength changed throughout the season, where colonies collected in mid-November (late season; November 11–19) were more interactive than colonies collected in October and early November (early season; October 7–November 7, Figure 5). For example, only  $27 \pm 16\%$  of the early season colonies with P-free CaCO<sub>3</sub> were grouped into “active” and “very active” categories compared with  $62 \pm 14\%$  of the late season colonies (Figure 5).

#### Colony morphotypes differ in their particle-interaction characteristics

We speculated that the day-to-day variations of interaction strength and selectivity (Figure 5) may reflect the co-occurrence of multiple *Trichodesmium* puff-shaped colony morphotypes. Two of these morphotypes, termed “thin” and “dense,” had distinct enough features to enable an easy visual separation (see STAR Methods). On November 17 and 19, we selected only thin and dense colonies and tested their interaction strength and selectivity to P-rich CaCO<sub>3</sub> particles (Figures 1 and 2). Indeed, these morphotypes exhibited markedly different particle-interaction characteristics (Figure 6A). Thin colonies formed strong interactions with both particles and were mostly grouped into “active” and “very active” categories (Figure 6A; 65% and 82% for P-free and P-rich CaCO<sub>3</sub>, respectively). On the other hand, dense colonies did not interact with particles, and a high proportion was grouped into the inactive and slightly active categories (Figure 6A; ~50% with both types of particles). The prevalence of these morphotypes in the Gulf of Aqaba changed during the season with thin colonies appearing later in the season. Given their contrasting particle-interaction characteristics, changes in their relative abundance within our experiments may partially translate into the observed day-to-day variations in their tendency to collect and retain particles (Figure 5). Different morphotype colonies also differ in their selectivity, with “thin” colonies showing selectivity and “dense” colonies showing no selectivity to P-rich particles (Figure 6A).

#### Assessing P limitation of natural colonies

Speculating that P limitation may be influencing their selectivity toward P-rich particles, we tested whether natural colonies are P-limited using the P stress marker gene *sphX* for multiple experimental days. We validated the marker as an indicator of P limitation by testing if *sphX* expression is downregulated in response to the addition of P during 24-h incubation. *SphX* expression levels dropped in colonies incubated with P



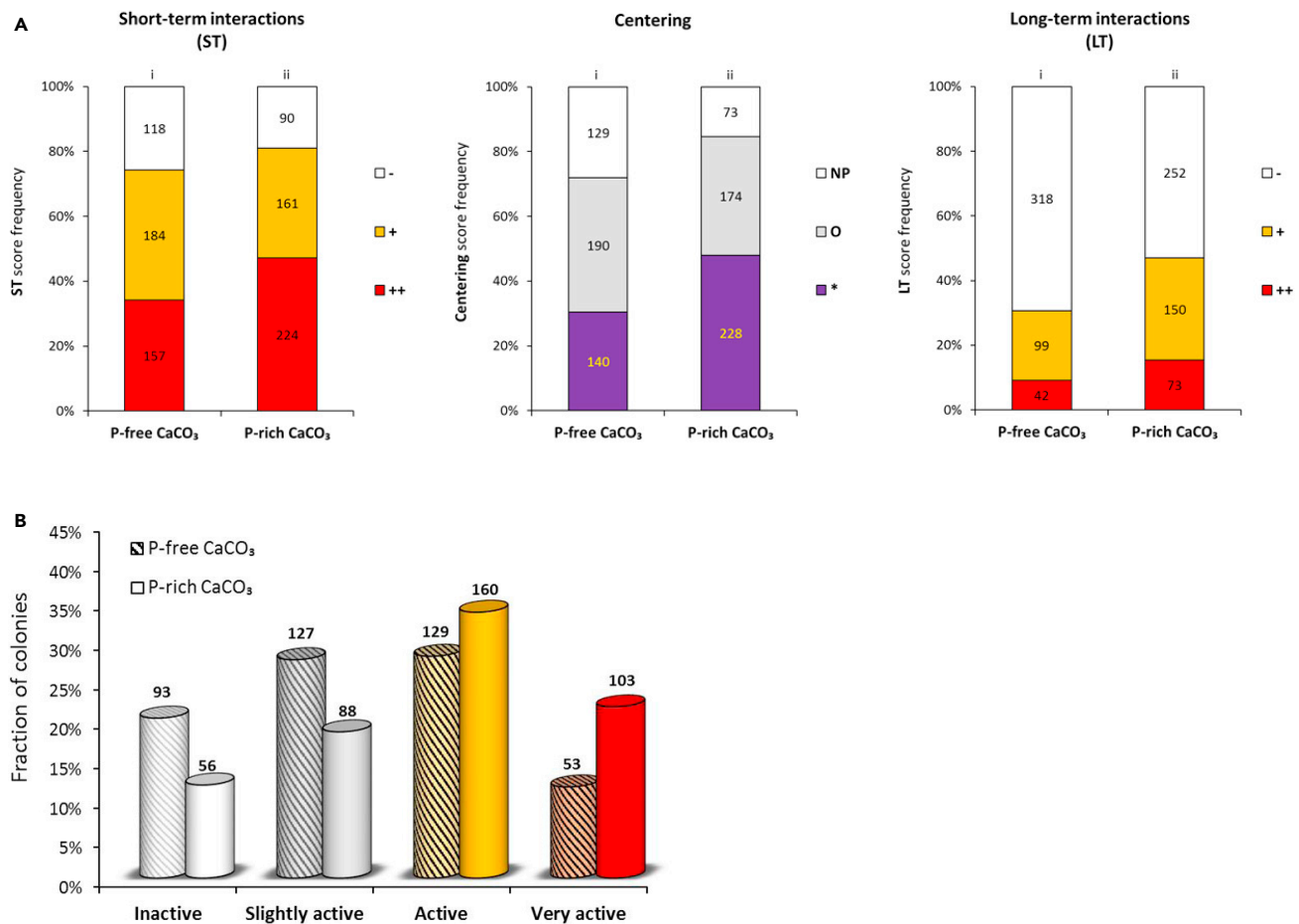


**Figure 4. Interactions between natural *Trichodesmium* colonies and P-free or P-rich CaCO<sub>3</sub> particles over the entire season as characterized by discrete parameters (A) and single colony index (B)**

(A) Short-term (ST) interactions, Centering, and Long-term (LT) interactions (see Figure 1). (B) Fraction of colonies per single-colony index category over the entire season (Figure 2). The color-coded categories are ordered at increasing interaction strength with “inactive” on the left and “very active” on the right. Hatched and solid bars represent P-free and P-rich CaCO<sub>3</sub> treatments, respectively. Numbers above each bar graph represent the total colony number in each category. A preference for P-rich CaCO<sub>3</sub> is seen by a higher abundance of colonies showing active patterns in the P-rich CaCO<sub>3</sub> treatment compared with the P-free CaCO<sub>3</sub> treatment.

(T<sub>24+P</sub>) compared with *in situ* colonies (T<sub>0</sub>) or colonies incubated without P (T<sub>24-P</sub>) (Figure 6B), indicating that the colonies were indeed P-limited. Unable to repeat such incubations owing to biomass limitation, we tested *in situ* colonies for *sphX* expression (T<sub>0</sub>) on 5 days throughout the bloom season (Figure 6C). On some of the days, *sphX* expression levels were as high as in the incubation experiment, whereas on other days it was slightly lower (Figure 6C). These data indicated that on some days (but not all days) natural colonies were P-limited but lacked the temporal resolution to resolve day-to-day variations in selectivity. Therefore, *sphX* expression could not link P limitation to the observed selection of P-rich particles. Nonetheless, *Trichodesmium* can access a range of dissolved organic P compounds through various enzymes (e.g., PhoA/PhoX; Orchard et al., 2009), and more work is required to explore the colony’s P stress comprehensively.

### Dust—the favorite mineral of natural *Trichodesmium* colonies

So far, we tested only P-free or P-rich CaCO<sub>3</sub>, whereas in nature, *Trichodesmium* colonies encounter more chemically and structurally complex particles like dust. Such particles contain multiple micro- and macro-nutrients required for the growth of *Trichodesmium*, which could be exploited by a sophisticated sensing and selecting behavior. In parallel, to mimic natural conditions, we incubated 10–20 natural colonies with desert dust on most experimental days (see STAR Methods).

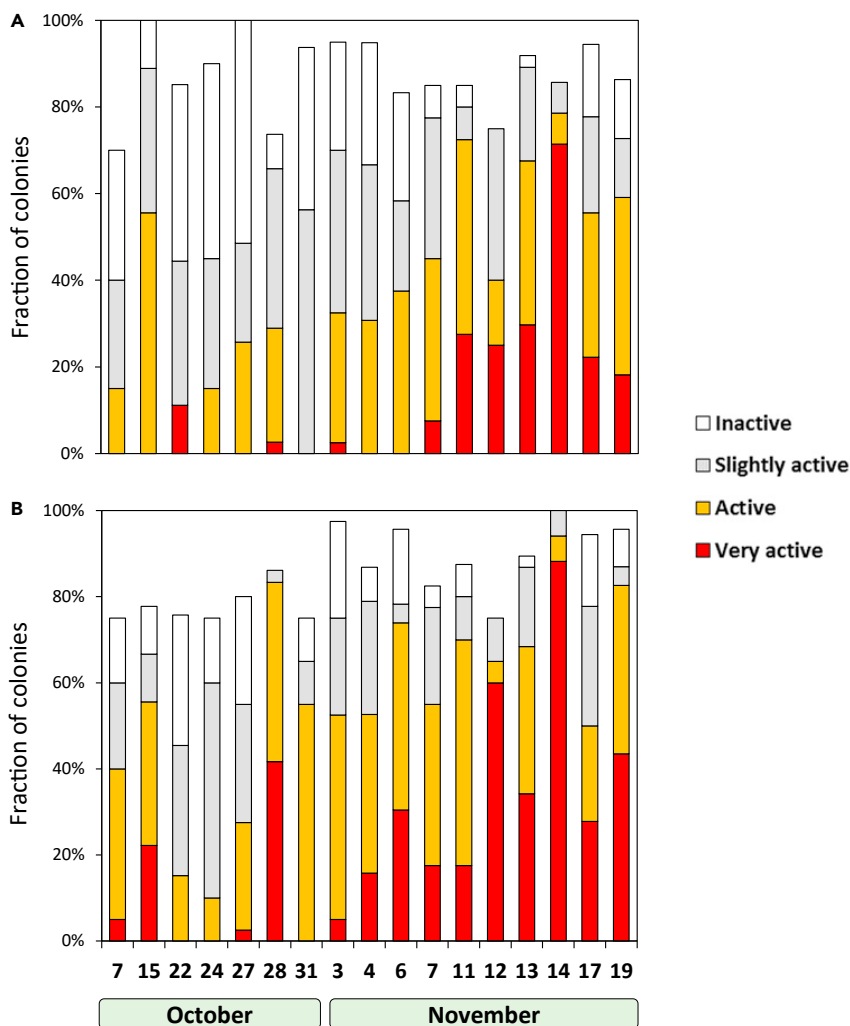


**Figure 5. Daily colony-particle interactions throughout the season presented using the single colony index**  
Day-to-day and seasonal variations of a colony's tendency to interact with particles (interaction strength) and preference for P-rich particles (selectivity). A high abundance of active colonies can be seen in late season (November 7–19) compared with more inactive colonies early in the season (October 7–November 7). Top (A) and bottom (B) panels represent P-free and P-rich  $\text{CaCO}_3$  treatments, respectively. Bars do not reach 100% as the missing fraction represents minor patterns that are not grouped into the four chosen categories.

The colony's strong preference for dust over both P-rich and P-free particles was consistent on all experimental days and in all experiments combined (Figures S2 and S3). When assessing the dust-incubated colonies using the single colony index, most colonies (~80%) could be placed in "active" and "very active" categories when incubated with dust in comparison with only 40% of the colonies incubated with P-free  $\text{CaCO}_3$  (Figure 7). Combined, *Trichodesmium* colonies typically interacted the strongest with dust, followed by P-rich  $\text{CaCO}_3$  and finally P-free  $\text{CaCO}_3$  particles.

## DISCUSSION

Our data demonstrate that natural Red Sea *Trichodesmium* colonies preferably interact, center, and retain  $\text{CaCO}_3$  particles coated with P in comparison with uncoated  $\text{CaCO}_3$  particles. This preference was observed for all interaction parameters on the population level (Figures 3 and 4A) and for the combined particle-interaction pathway of individual colonies (Figures 4B, 6A, 7, and 8), indicating that *Trichodesmium* colonies can discern the presence or absence of P on particles. Furthermore, the colonies clearly favored dust over all other particles tested (Figure 7). Together with Kessler et al. (2020a), our study suggests that



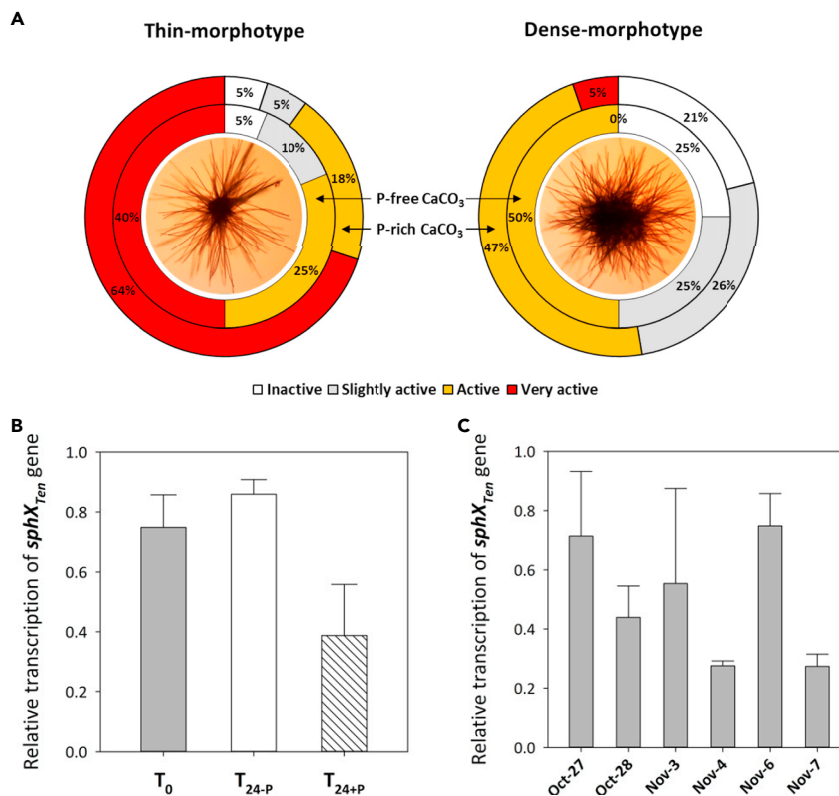


**Figure 6. Factors influencing the day-to-day variability in colony-particle interactions**

(A) Separation of thin (left) and dense (right) morphotypes on November 17 and 19 demonstrates differences of a colony's tendency to interact with particles (interaction strength) and preference for P-rich particles (selectivity) according to morphotype. Interaction strength is based on the single colony index categories, whereas selectivity is based on differences between the inner (P-free CaCO<sub>3</sub>) and outer (P-rich CaCO<sub>3</sub>) circles. In general, thin morphotypes were more interactive (interaction strength) and showed more selectivity for particles in comparison with the dense morphotypes. (B) Relative expressions of P stress marker gene *sphX* in natural colonies, collected on November 6, *in situ* (T<sub>0</sub>) and after 24 h incubations without PO<sub>4</sub><sup>3-</sup> (T<sub>24-P</sub>) and with 5 μM PO<sub>4</sub><sup>3-</sup> (T<sub>24+P</sub>). The lower transcription of *sphX* gene transcription for T<sub>24+P</sub> in comparison with T<sub>0</sub> and T<sub>24-P</sub> indicates that the collected colonies were P-limited. Error bars represent the standard deviation (n = 2).

(C) Relative expressions of *sphX* in natural colonies, collected *in situ* for 6 days throughout the season (including November 6). Colonies collected on October 27 and November 3 were presumably P-limited owing to similar *sphX* expression in comparison with November 6. Error bars represent the standard deviation (n = 2).

*Trichodesmium* can (1) chemically sense nutrient content of particles and (2) modify its interactions with particles to optimize collection and retention of nutrient-rich particles.

### Physiological and ecological factors affecting *Trichodesmium*-particle interactions

The newly observed ability of colonies to sense and select P-rich particles is nested within a broader colony-particle behavior that includes initial adhesion, centering, or removal of particles and their retention within the colony core (Figures 1, 3, and 4). Variations in both interaction strength and selectivity were observed among discrete experimental days and during the season (Figure 5), providing grounds for exploring the potential factors driving colony-particle interactions.

#### Variations among colony morphotypes in interactions with particles

Variations among individual colonies within a single day and among different days regarding both interaction strength and selectivity (Figures 3, 5, and 8) may originate from the co-occurrence of morphotypes that differ in their tendency to interact with particles. We observed strong differences among two common morphotypes: "thin" colonies with a strong tendency to interact and retain particles and "dense" colonies that were mostly inactive (Figure 6A). Although these are not the only morphotypes present in the Gulf of

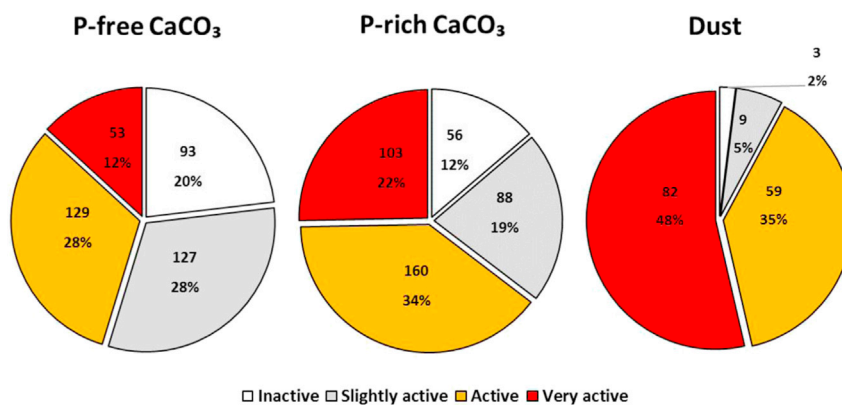


**Figure 7. Summary of colony-particle interactions observed in this study for all tested mineral types (P-free CaCO<sub>3</sub>, P-rich CaCO<sub>3</sub>, and mineral dust) according to the single colony index categories**

Collectively a total of 1,104 colonies were characterized in this study and 962 colonies following common patterns were presented above. Colonies show a strong preference for dust over P-rich CaCO<sub>3</sub> as well as discrimination against P-free CaCO<sub>3</sub>.

Aqaba, the higher abundance of “thin” colonies toward the end of the bloom season most likely explains the increase in the observed interaction strength (Figure 5). The contrast observed here between the two morphotypes offers a good basis to explore the molecular and biochemical components involved in the ability to adhere to particles and shuffle them along the filaments. Extrapolating our findings to other environments, it is important to note that not all colony-forming *Trichodesmium* species will equally interact with dust and utilize it as a source for nutrients such as P and Fe.

#### Interaction strength and selectivity are linked

Although some of the daily variability in colony-particle interactions can be accounted for by the observed differences in morphotype, other factors such as the colony life stage, position in the water column, and microbial consortium composition are also likely to be of influence. Our experiments did not examine these options, but we observed a link between interaction strength and selectivity, which may provide some insights on this complex behavior. Selectivity for P-rich particles was most pronounced on days where the interaction strength was intermediate, whereas selectivity was less pronounced on days where the interaction strength was either minimal or maximal (Figure 8). For example, on October 22, over 80% of the colonies followed inactive to slightly active categories and did not prefer any of the particles (Figure 8). This trend is easy to reconcile as no selection is expected when colonies do not interact with particles. Assuming that *Trichodesmium* use particles as a source of nutrients (Basu et al., 2019), days with low interaction and low selectivity may comprise colonies that are not relying on particles to supply their nutritional demand. On the other hand, highly interactive colonies exhibiting low selectivity are exemplified by data from November 14 (Figure 8). In such cases, the strong tendency to collect particles may mask the colony’s ability to distinguish between particles. In nutrient terms, these days may contain nutrient-starved colonies (i.e., “beggars can’t be choosers”). Among these two extremes, many experimental days, such as November 6, were characterized by intermediate interaction strength but high selectivity (Figures 8 and S4). We observed that colonies on November 6 were P-limited (based on *sphX* expressions, Figure 6B), but as discussed below, more research is required to untangle the link between colony’s nutrient requirements and interactions with particles.

#### P limitation does not fully explain particle interaction and retention

We propose that the reported ability to selectively collect P-rich particles is an important mechanism enabling *Trichodesmium* to maximize its capacity to obtain P from dust and other particles in seawater. Red Sea colonies used in several of our experiments were P-stressed, as evidenced by high expression levels of the P stress marker-gene *sphX* (Figure 6B), potentially providing a “motivation” for selecting P-rich particles. Nonetheless, we did not find a link between the colony’s P-nutrition or P-flux and their interaction with particles.

In our incubations, colonies can retain both dust and P-coated particles up to 27 h (e.g., Figure 3) despite the provision of a sufficient flux of P from these particles. Based on concentrations of added particles and

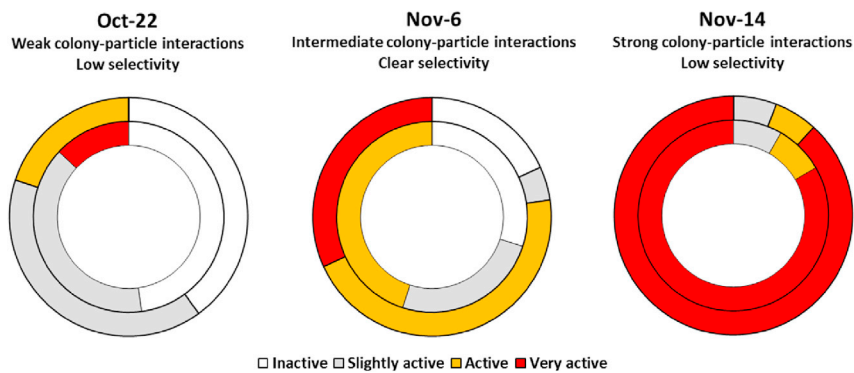


**Figure 8. Contrasting colony-particle interaction days**

Three days with contrasting colony-particle interaction strength to demonstrate variations in a colony's tendency to interact with particles (interaction strength) and preference for P-rich particles (selectivity). Interaction strength is based on the single colony index categories, whereas selectivity is based on differences between the inner (P-free  $\text{CaCO}_3$ ) and outer (P-rich  $\text{CaCO}_3$ ) circles.

rates of P dissolution from dust or P desorption from P-coated  $\text{CaCO}_3$ , we calculated that 0.05 to 0.49  $\mu\text{M}$   $\text{PO}_4^{3-}$  accumulated in each well within 3 h (Table S5). These P concentrations greatly exceed the colony's P-requirements (Sañudo-Wilhelmy et al., 2001, 2004), and hence it is safe to assume that colonies became P-replete within few hours from addition of P-rich  $\text{CaCO}_3$  or dust. We also tested if P addition prior to the incubation will stop colonies from interacting with particles. Pre-incubating colonies with 5  $\mu\text{M}$   $\text{PO}_4^{3-}$  for 2 h on two separate days yielded no to low effect on initial interaction and centering of dust (Figure S5).

We were further unable to link the seasonal change in P supply in the Gulf of Aqaba with interaction patterns. During autumn, as surface waters cool down, convective mixing gradually increases P supply from the phosphocline to the mixed layer (Torfstein et al., 2020). Assuming that mixing of "deep"  $\text{PO}_4^{3-}$  is an important P source for *Trichodesmium*, colonies are expected to be less P-limited in late autumn. Contrary to the seasonal change in P supply, the interaction strength increased throughout the season (Figure 5). Our findings therefore do not support that P limitation leads colonies to "activate" their particle collection behavior. Nonetheless, as *Trichodesmium* is often limited or co-limited by nutrients other than P such as Fe and other trace elements (Chappell et al., 2012; Held et al., 2020b; Ho, 2013; Mills et al., 2004; Moore et al., 2009), our ability to draw conclusions on the drivers of particle collection behavior is limited and more research is required to explore this avenue.

#### Interactions with nutrient-free minerals

Although colonies prefer P-rich  $\text{CaCO}_3$ , many colonies interacted initially with nutrient-free  $\text{CaCO}_3$  (74%; Figure 4A, [+ and ++, ST-scores]), possibly indicating that particles serve additional roles in a colony's ecology. However, over time, the fraction of colonies that actively centered or retained these non-nutritional particles dropped significantly (31% LT-scores). These trends, thus, reveal that *Trichodesmium*'s particle selection "system" requires several hours of fine-tuning until they are left with "valuable" particles. Such a time span may be expected when considering that a complex mechanism involving both chemical sensing and particle translocation must be activated in order for these selective-particle interactions to take place.

#### Optimization of particle retention within the colony's core through particle removal

During the overnight incubation, many colonies removed some of the particles they originally captured (Figures 3 and 4A). This phenomenon may partly result from an overload of particles at the start of incubation that were subsequently lost over time. However, the sharp contrast between the particle-loaded core and the particle-free periphery observed by Nano-SIMS analysis of *in situ* Red Sea colonies by Kessler et al. (2020a) is indicative of an active and controlled particle translocation mechanism. The removal of particles was also shown to be a selective process as dust was removed to a lesser degree than P or Fe-rich minerals, whereas nutrient-free  $\text{CaCO}_3$  and silica minerals were removed to the greatest extent (Figures 3, 4A and 9; Kessler et al., 2020a, Figure 4).

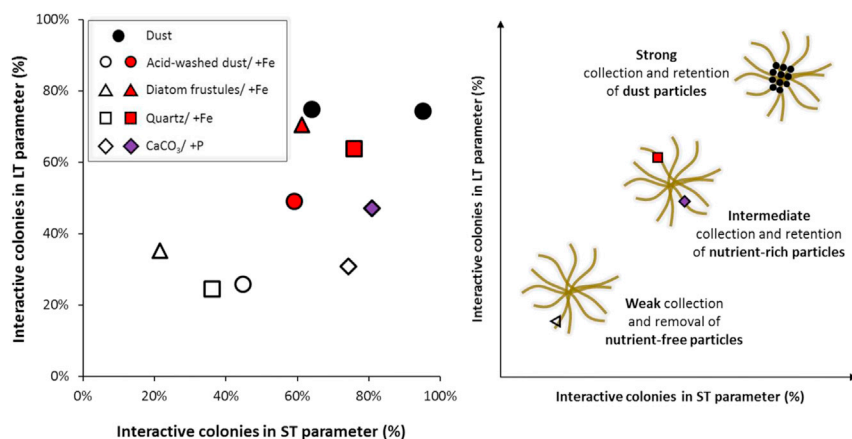


**Figure 9. Compilation of *Trichodesmium* colony-particle interaction studies**

We combine the current study data with that of Kessler et al. (2020a), by plotting the percentage of colonies interacting with particles initially (ST) and after overnight incubation (LT). Nutrient-free particles ( $\text{CaCO}_3$ , quartz, diatom frustule, and acid-cleaned dust) are plotted as empty symbols, nutrient-rich particles appear as colored symbols, and dust appear as black circles. A clear selection can be seen among different mineral types, where the cartoon on the right highlights key trends from the data.

The centering and removal of particles can hereby be viewed as two edges of the same behavior, a negative and a positive one, both involving the chemical “sensing” of the mineral composition and subsequent activation of cellular mechanisms leading to particle translocation. These two processes, on the other hand, likely differ in their coordination level, as the simple detachment of filaments can lead to particle loss while a coordinated motion of several filaments is required in order to push particles to the colony core (Rubin et al., 2011).

The ability to remove particles provides flexibility with regards to the amount and type of particles colonies can retain. Such flexibility enables colonies to offset the potential negative effects of a high particle load such as buoyancy loss, exposure to toxic trace elements present in dust, increased visibility to predators, self-shading by particles, and restricted diffusion of solutes (Held et al., 2020a; Kessler et al., 2020b; Paytan et al., 2009; Walsby, 1992). An ability to remove particles also enables colonies to rapidly change their pool of particles and replace nutrient-exhausted particles with fresh ones, potentially providing larger nutrient fluxes. The documented ability to control the amount (and possibly type) of particles may hereby explain a recent report by Held et al., (2020a), who collected both particle-free and particle-loaded colonies from a single net tow in the Caribbean Sea (Held et al., 2020a).

#### Mineral-collection ranking—*Trichodesmium* colonies prefer dust over all minerals

Our study complements the work conducted by Kessler et al., 2020a and together can shed light on the complex behavior of particle collection and the role of dust as a nutrient source to *Trichodesmium*. Each study examined a different set of minerals, but both included interactions with natural dust. Seeking to integrate both studies, we plotted the percentage of colonies that positively interacted with each of the nine different particle types at the beginning (ST) and end (LT) of the incubation (Figure 9). Combined, our studies clearly identify natural dust as the most favorable particle type with 65%–95% of the colonies interacting with it (Figure 9, top-right corner). The least favored particles were the nutrient-free minerals, including quartz, diatom frustules,  $\text{CaCO}_3$ , and acid-cleaned dust, with only 20%–35% of the colonies interacting with these minerals (Figure 9, bottom-left corner). Nutrient-rich minerals from both studies, including P-adsorbed  $\text{CaCO}_3$  and three Fe-coated minerals showed intermediate rates of particle interaction, with 50%–80% of the colonies interacting with these minerals (Figure 9, center). Although these studies were conducted 3 years apart and in different seasons, one in spring and another in autumn, probably comprised different colony morphotypes (or even different *Trichodesmium* species), and applied different local desert dust samples, the fraction of colonies retaining dust after overnight incubation (LT) was surprisingly similar (Figure 9, ST criteria differ between studies preventing exact comparison). The quantitative agreement between our studies indicate that Red Sea colonies-dust interactions are robust,

making our findings applicable to additional oceanic environments. Indeed, several recent studies from the South Atlantic and Caribbean Sea reported the significant accumulation of mineral particles by natural colonies (Bif and Yunes, 2017; Held et al., 2020a).

Our studies independently reveal that colonies can discern the presence of either P or Fe on particles and selectively collect minerals containing these elements. When considering dust as a source of P and Fe to *Trichodesmium*, these elements share some similarities but also exhibit important differences. Dust contains relatively high Fe concentrations (3.5 wt%; Duce and Tindale, 1991; Mahowald et al., 2005) compared with P (0.03–0.20 wt%; Stockdale et al., 2016; Zhang et al., 2018). This is in contrast to the ~80-fold higher cellular requirements for P compared with Fe (Sañudo-Wilhelmy et al., 2001, 2004). Despite the low overall solubility of both Fe and P from dust, typically estimated 0.1%–10% (Aguilar-Islas et al., 2010; Mahowald et al., 2005, 2008; Stockdale et al., 2016), *Trichodesmium* can employ a variety of biochemical pathways and physical mechanisms in order to enhance the solubility and bioavailability of Fe from dust (Basu et al., 2019; Basu and Shaked, 2018; Eichner et al., 2019, 2020; Held et al., 2020a; Kessler et al., 2020b; Rubin et al., 2011). The effect of such mechanisms on dust-P solubility has not yet been studied, but as P is often associated with Fe, it is likely that *Trichodesmium* can also modify dust-P and enhance its bioavailability.

The colonies' clear preference for dust in comparison with all other minerals (Figures 7 and 9) may involve both physical and chemical characteristics of dust. Natural dust and aerosols contain differently sized single and aggregated particles, varying in shape and surface roughness (Genga et al., 2018; Kessler et al., 2020b; Marcotte et al., 2020), potentially making it easier to translocate and center in comparison with some of the homogeneous smooth minerals that were used. In addition, dust may contain nutrients other than P or Fe, such as additional trace metals, organic matter, and bacteria (Chen et al., 2007; Herut et al., 2016; Torfstein et al., 2017). More research is required to unfold the drivers and pathways involved in *Trichodesmium*-dust interactions; nonetheless, the mere ability of selectively collecting particles bears significant environmental significance. The selection of particles enables *Trichodesmium* colonies to optimize the collection and retention of dust to favor particles that can supply them with scarce Fe and P and consequently contribute to nutrient cycling and productivity in the ocean. The importance of *Trichodesmium* in fueling the ocean with nutrients is expected to further increase as its abundance expands in the warming ocean (Tang et al., 2020), which is projected to receive higher dust fluxes (Meskhidze et al., 2005).

## Conclusion

In this study, we assessed the particle collection behavior of *Trichodesmium* by incubating ~1,200 natural Red Sea colonies with P-free and P-rich CaCO<sub>3</sub> and dust over 17 individual days during autumn of 2019. We documented a new ability of *Trichodesmium* to preferably collect, center, and retain P-rich particles in the colony core while removing P-free particles. Zooming into day-to-day variations in colony-particle interactions, we examined three possible factors influencing these interactions: (1) differences between colony morphotypes, (2) varying degree of colony P limitation, and (3) dependency between interaction strength and selectivity. We found that morphotypes differed in their tendency to interact with particles regardless of their P-nutritional status and that the colony's tendency to interact with particles was linked to their selectivity to P-rich particles. Combining our findings with that of Kessler et al. (2020a), we found that: (1) Fe- and P-rich minerals are preferred over nutrient-free particles, indicating that natural *Trichodesmium* colonies have the ability to sense the presence of nutrients on particles and accordingly modify their behavior. (2) Dust is preferred over Fe- and P-rich minerals, suggesting that *Trichodesmium* may require additional nutrients from the dust. The ability to selectively collect nutritional particles contributes to *Trichodesmium*'s ecological success with subsequent effects on global C and N<sub>2</sub> fixation in the ocean.

## Limitations of the study

The interactions between *Trichodesmium* and particles described here are extremely complex and highly dynamic, and hence it is hard to fully resolve the underlying mechanisms controlling colony-particle interactions. The choice of experimenting with natural colonies adds another level of complication and restricts our ability to explain variations among days and between two morphotypes of colonies. In addition, stereoscopic observations by naked eyes by different individuals may result in some biases (that were partly resolved by randomization). Other drawbacks of the stereoscope include low resolution that restricts observation for relatively large particles (>10 μm), missing interactions with smaller particles. The long observation time restricts the number of time points, potentially missing important shifts in the interactions.

## STAR★METHODS

Detailed methods are provided in the online version of this paper and include the following:

- KEY RESOURCES TABLE
- RESOURCE AVAILABILITY
  - Lead contact
  - Materials availability
  - Data and code availability
- EXPERIMENTAL MODEL AND SUBJECT DETAILS
  - *Trichodesmium* IMS101 culture
- METHOD DETAILS
  - Experiment overview
  - Colony collection
  - Particle preparation and description
  - Determination of colony-particle interactions
  - Examination of P stress in natural colonies
  - Compilation of particle selection studies
- QUANTIFICATION AND STATISTICAL ANALYSES

## SUPPLEMENTAL INFORMATION

Supplemental information can be found online at <https://doi.org/10.1016/j.isci.2021.103587>.

## ACKNOWLEDGMENTS

We sincerely thank Murielle Dray (IUI), Emanuel Sestieri (IUI), and Prof. Haizheng Hong (Xiamen University) for valuable assistance during the study. Y.S. and D.S.'s groups were co-funded by ISF-NSFC joint research program (Grant No. 2398/18). Y.S.'s group was specifically funded by ISF (260/21). D.S. and F.Z. were specifically supported by NSFC (31861143022) and that portion of work was conducted in Xiamen University. S.W. acknowledges CSC-HUJI doctoral fellowship and F.Z. acknowledges PBC Postdoctoral fellowship. S.W. thanks Dr. Yumin Kan and Dr. Chao Wang for their useful comments on this manuscript.

## AUTHOR CONTRIBUTIONS

S.W. and Y.S. conceived the project and planned experiments. S.W. prepared P-free/P-coated CaCO<sub>3</sub> and characterized their P release into seawater. S.W., C.K., N.K., and M.E. performed incubation experiments of *Trichodesmium* colonies with particles. F.Z. and S.W. conducted qPCR work in D.S.'s lab. S.W., F.Z., N.K., and Y.S. analyzed the data and created the figures. S.W., C.K., and Y.S. drafted the manuscript and finalized it with all other authors. Y.S. and D.S. supervised the entire study.

## DECLARATION OF INTERESTS

The authors declare that they have no conflict of interest.

Received: June 16, 2021

Revised: October 1, 2021

Accepted: December 6, 2021

Published: January 21, 2022

## REFERENCES

- Aguilar-Islas, A.M., Wu, J., Rember, R., Johansen, A.M., and Shank, L.M. (2010). Dissolution of aerosol-derived iron in seawater: Leach solution chemistry, aerosol type, and colloidal iron fraction. *Mar. Chem.* 120, 25–33. <https://doi.org/10.1016/j.marchem.2009.01.011>.
- Ammerman, J.W., Hood, R.R., Case, D.A., and Cotner, J.B. (2003). Phosphorus deficiency in the Atlantic: An emerging paradigm in oceanography. *Eos, Trans. Am. Geophys. Union* 84, 165–170. <https://doi.org/10.1029/2003EO180001>.
- Anderson, L.D., Faul, K.L., and Paytan, A. (2010). Phosphorus associations in aerosols: What can they tell us about P bioavailability? *Mar. Chem.* 120, 44–56. <https://doi.org/10.1016/j.marchem.2009.04.008>.
- Barkley, A.E., Prospero, J.M., Mahowald, N., Hamilton, D.S., Popendorf, K.J., Oehlert, A.M., Pourmand, A., Gatineau, A., Panechou-Pulcherie, K., Blackwelder, P., and Gaston, C.J. (2019). African biomass burning is a substantial source of phosphorus deposition to the Amazon, Tropical Atlantic Ocean, and Southern Ocean. *Proc. Natl. Acad. Sci. U. S. A.* 116, 16216–16221. <https://doi.org/10.1073/pnas.1906091116>.
- Basu, S., Gledhill, M., de Beer, D., Prabhu Matondkar, S.G., and Shaked, Y. (2019). Colonies of marine cyanobacteria *Trichodesmium* interact with associated bacteria to acquire iron from



- dust. *Commun. Biol.* 2, 1–8. <https://doi.org/10.1038/s42003-019-0534-z>.
- Basu, S., and Shaked, Y. (2018). Mineral iron utilization by natural and cultured *Trichodesmium* and associated bacteria. *Limnol. Oceanogr.* 63, 2307–2320. <https://doi.org/10.1002/lno.10939>.
- Bergman, B., Sandh, G., Lin, S., Larsson, J., and Carpenter, E.J. (2013). *Trichodesmium* a widespread marine cyanobacterium with unusual nitrogen fixation properties. *FEMS Microbiol. Rev.* 37, 286–302. <https://doi.org/10.1111/j.1574-6976.2012.00352.x>.
- Berman-Frank, I., Lundgren, P., Chen, Y.B., Küpper, H., Kolber, Z., Bergman, B., and Falkowski, P. (2001). Segregation of nitrogen fixation and oxygenic photosynthesis in the marine cyanobacterium *Trichodesmium*. *Science* 294, 1534–1537. <https://doi.org/10.1126/science.1064082>.
- Bif, M.B., and Yunes, J.S. (2017). Distribution of the marine cyanobacteria *Trichodesmium* and their association with iron-rich particles in the South Atlantic Ocean. *Aquat. Microb. Ecol.* 78, 107–119. <https://doi.org/10.3354/ame01810>.
- Bopp, L., Resplandy, L., Orr, J.C., Doney, S.C., Dunne, J.P., Gehlen, M., Halloran, P., Heinze, C., Ilyina, T., Séférian, R., et al. (2013). Multiple stressors of ocean ecosystems in the 21st century: projections with CMIP5 models. *Biogeosciences* 10, 6225–6245. <https://doi.org/10.5194/bg-10-6225-2013>.
- Capone, D.G., and Carpenter, E.J. (1982). Nitrogen fixation in the marine environment. *Science* 217, 1140–1142. <https://doi.org/10.1016/B978-0-12-372522-6.00004-9>.
- Capone, D.G., Zehr, J.P., Paerl, H.W., Bergman, B., and Carpenter, E.J. (1997). *Trichodesmium*, a globally significant marine cyanobacterium. *Science* 276, 1221–1229. <https://doi.org/10.1126/science.276.5316.1221>.
- Chappell, P.D., Moffett, J.W., Hynes, A.M., and Webb, E.A. (2012). Molecular evidence of iron limitation and availability in the global diazotroph *Trichodesmium*. *ISME J.* 6, 1728–1739. <https://doi.org/10.1038/ismej.2012.13>.
- Chappell, P.D., and Webb, E.A. (2010). A molecular assessment of the iron stress response in the two phylogenetic clades of *Trichodesmium*. *Environ. Microbiol.* 12, 13–27. <https://doi.org/10.1111/j.1462-2920.2009.02026.x>.
- Chen, Y., Mills, S., Street, J., Golan, D., Post, A., Jacobson, M., and Paytan, A. (2007). Estimates of atmospheric dry deposition and associated input of nutrients to Gulf of Aqaba seawater. *J. Geophys. Res. Atmos.* 112, 1–14. <https://doi.org/10.1029/2006JD007858>.
- Chen, Y., Tovar-Sanchez, A., Siefert, R.L., Sañudo-Wilhelmy, S.A., and Zhuang, G. (2011). Luxury uptake of aerosol iron by *Trichodesmium* in the western tropical North Atlantic. *Geophys. Res. Lett.* 38. <https://doi.org/10.1029/2011GL048972>.
- Chien, C. Te, Mackey, K.R.M., Dutkiewicz, S., Mahowald, N.M., Prospero, J.M., and Paytan, A. (2016). Effects of African dust deposition on phytoplankton in the western tropical Atlantic Ocean off Barbados. *Glob. Biogeochem. Cycles* 30, 716–734. <https://doi.org/10.1002/2015GB005334>.
- Deutsch, C., Sarmiento, J.L., Sigman, D.M., Gruber, N., and Dunne, J.P. (2007). Spatial coupling of nitrogen inputs and losses in the ocean. *Nature* 445, 163–167. <https://doi.org/10.1038/nature05392>.
- Duce, R.A., and Tindale, N.W. (1991). Atmospheric transport of iron and its deposition in the ocean. *Limnol. Oceanogr.* 36, 1715–1726.
- Dyhrman, S.T., Chappell, P.D., Haley, S.T., Moffett, J.W., Orchard, E.D., Waterbury, J.B., and Webb, E.A. (2006). Phosphonate utilization by the globally important marine diazotroph *Trichodesmium*. *Nature* 439, 68–71. <https://doi.org/10.1038/nature04203>.
- Dyhrman, S.T., Webb, E.A., Anderson, D.M., Moffett, J.W., and Waterbury, J.B. (2002). Cell-specific detection of phosphorus stress in *Trichodesmium* from the Western North Atlantic. *Limnol. Oceanogr.* 47, 1832–1836. <https://doi.org/10.4319/lo.2002.47.6.1832>.
- Eichner, M., Basu, S., Gledhill, M., de Beer, D., and Shaked, Y. (2019). Hydrogen dynamics in *Trichodesmium* colonies and their potential role in mineral iron acquisition. *Front. Microbiol.* 10, 1565. <https://doi.org/10.3389/fmicb.2019.01565>.
- Eichner, M., Basu, S., Wang, S., de Beer, D., and Shaked, Y. (2020). Mineral iron dissolution in *Trichodesmium* colonies: The role of O<sub>2</sub> and pH microenvironments. *Limnol. Oceanogr.* 65, 1149–1160. <https://doi.org/10.1002/lno.11377>.
- Fernández, A., Mouriño-Carballido, B., Bode, A., Varela, M., and Marañón, E. (2010). Latitudinal distribution of *Trichodesmium* spp. and N<sub>2</sub> fixation in the Atlantic Ocean. *Biogeosciences* 7, 3167–3176. <https://doi.org/10.5194/bg-7-3167-2010>.
- Frischkorn, K.R., Haley, S.T., and Dyhrman, S.T. (2018). Coordinated gene expression between *Trichodesmium* and its microbiome over day-night cycles in the North Pacific Subtropical Gyre. *ISME J.* 12, 997–1007. <https://doi.org/10.1038/s41396-017-0041-5>.
- Fuller, N.J., West, N.J., Marie, D., Yallop, M., Rivlin, T., Post, A.F., and Scanlan, D.J. (2005). Dynamics of community structure and phosphate status of picocyanobacterial populations in the Gulf of Aqaba, Red Sea. *Limnol. Oceanogr.* 50, 363–375. <https://doi.org/10.4319/lo.2005.50.1.0363>.
- Genga, A., Siciliano, T., Siciliano, M., Aiello, D., and Tortorella, C. (2018). Individual particle SEM-EDS analysis of atmospheric aerosols in rural, urban, and industrial sites of Central Italy. *Environ. Monit. Assess.* 190, 456. <https://doi.org/10.1007/s10661-018-6826-9>.
- Gross, A., Reichmann, O., Zarka, A., Weiner, T., Be’eri-Shlevin, Y., and Angert, A. (2020). Agricultural sources as major supplies of atmospheric phosphorus to Lake Kinneret. *Atmos. Environ.* 224, 117207. <https://doi.org/10.1016/j.atmosenv.2019.117207>.
- Held, N.A., Sutherland, K.M., Webb, E.A., McIlvin, M.R., Cohen, N.R., Devaux, A.J., Hutchins, D.A., Waterbury, J.B., Hansel, C.M., and Saito, M.A. (2020a). Mechanisms and heterogeneity of mineral use by natural colonies of the cyanobacterium *Trichodesmium*. *bioRxiv*, 1–13. <https://doi.org/10.1101/2020.09.24.295147>.
- Held, N.A., Webb, E.A., McIlvin, M.M., Hutchins, D.A., Cohen, N.R., Moran, D.M., Kunde, K., Lohan, M.C., Mahaffey, C., Malcolm, E., and Saito, M.A. (2020b). Co-occurrence of Fe and P stress in natural populations of the marine diazotroph *Trichodesmium*. *Biogeosciences* 17, 2537–2551. <https://doi.org/10.5194/bg-17-2537-2020>.
- Herut, B., Rahav, E., Tsarakaki, T.M., Giannakourou, A., Tsiola, A., Psarra, S., Lagaria, A., Papageorgiou, N., Mihalopoulos, N., Theodosi, C.N., et al. (2016). The potential impact of Saharan dust and polluted aerosols on microbial populations in the East Mediterranean Sea, an overview of a mesocosm experimental approach. *Front. Mar. Sci.* 3, 226. <https://doi.org/10.3389/fmars.2016.00226>.
- Ho, T.Y. (2013). Nickel limitation of nitrogen fixation in *Trichodesmium*. *Limnol. Oceanogr.* 58, 112–120. <https://doi.org/10.4319/lo.2013.58.1.0112>.
- Hynes, A.M., Chappell, P.D., Dyhrman, S.T., Doney, S.C., and Webb, E.A. (2009). Cross-basin comparison of phosphorus stress and nitrogen fixation in *Trichodesmium*. *Limnol. Oceanogr.* 54, 1438–1448. <https://doi.org/10.4319/lo.2009.54.1438>.
- Jickells, T.D., An, Z.S., Andersen, K.K., Baker, A.R., Bergametti, G., Brooks, N., Cao, J.J., Boyd, P.W., Duce, R.A., Hunter, K.A., et al. (2005). Global iron connections between desert dust, ocean biogeochemistry, and climate. *Science* 308, 67–71. <https://doi.org/10.1126/science.1105959>.
- Johnson, M.S., Meskhidze, N., Solmon, F., Gassó, S., Chuang, P.Y., Gaiero, D.M., Yantosca, R.M., Wu, S., Wang, Y., and Carouge, C. (2010). Modeling dust and soluble iron deposition to the South Atlantic Ocean. *J. Geophys. Res. Atmos.* 115, 1–13. <https://doi.org/10.1029/2009JD013311>.
- Karl, D.M. (2014). Microbially mediated transformations of phosphorus in the sea: New views of an old cycle. *Ann. Rev. Mar. Sci.* 6, 279–337. <https://doi.org/10.1146/annurev-marine-010213-135046>.
- Karl, D.M. (2000). Phosphorus, the staff of life. *Nature* 406, 31–33. <https://doi.org/10.1038/35017683>.
- Kessler, N., Armoza-Zvuloni, R., Wang, S., Basu, S., Weber, P.K., Stuart, R.K., and Shaked, Y. (2020a). Selective collection of iron-rich dust particles by natural *Trichodesmium* colonies. *ISME J.* 14, 91–103. <https://doi.org/10.1038/s41396-019-0505-x>.
- Kessler, N., Kraemer, S.M., Shaked, Y., and Schenkvelld, W.D.C.C. (2020b). Investigation of siderophore-promoted and reductive dissolution of dust in marine microenvironments such as *Trichodesmium* colonies. *Front. Mar. Sci.* 7, 1–15. <https://doi.org/10.3389/fmars.2020.00045>.
- Kuhn, A.M., Fennel, K., and Berman-Frank, I. (2018). Modelling the biogeochemical effects of heterotrophic and autotrophic N<sub>2</sub> fixation in the Gulf of Aqaba (Israel), Red Sea. *Biogeosciences*

15, 7379–7401. <https://doi.org/10.5194/bg-15-7379-2018>.

Langlois, R.J., Mills, M.M., Ridame, C., Croot, P., and LaRoche, J. (2012). Diazotrophic bacteria respond to Saharan dust additions. *Mar. Ecol. Prog. Ser.* 470, 1–14. <https://doi.org/10.3354/meps10109>.

Lenes, J.M., Darrow, B.A., Walsh, J.J., Prospero, J.M., He, R., Weisberg, R.H., Vargo, G.A., and Heil, C.A. (2008). Saharan dust and phosphatic fidelity: A three-dimensional biogeochemical model of *Trichodesmium* as a nutrient source for red tides on the West Florida Shelf. *Cont. Shelf Res.* 28, 1091–1115. <https://doi.org/10.1016/j.csr.2008.02.009>.

Mackey, K.R.M., Labiosa, R.G., Calhoun, M., Street, J.H., Post, A.F., and Paytan, A. (2007). Phosphorus availability, phytoplankton community dynamics, and taxon-specific phosphorus status in the Gulf of Aqaba, Red Sea. *Limnol. Oceanogr.* 52, 873–885. <https://doi.org/10.4319/lo.2007.52.2.0873>.

Mackey, K.R.M., Roberts, K., Lomas, M.W., Saito, M.A., Post, A.F., and Paytan, A. (2012). Enhanced solubility and ecological impact of atmospheric phosphorus deposition upon extended seawater exposure. *Environ. Sci. Technol.* 46, 10438–10446. <https://doi.org/10.1021/es3007996>.

Mahowald, N., Jickells, T.D., Baker, A.R., Artaxo, P., Benitez-Nelson, C.R., Bergametti, G., Bond, T.C., Chen, Y., Cohen, D.D., Herut, B., et al. (2008). Global distribution of atmospheric phosphorus sources, concentrations and deposition rates, and anthropogenic impacts. *Glob. Biogeochem. Cycles* 22. <https://doi.org/10.1029/2008GB003240>.

Mahowald, N.M., Baker, A.R., Bergametti, G., Brooks, N., Duce, R.A., Jickells, T.D., Kubilay, N., Prospero, J.M., and Tegen, I. (2005). Atmospheric global dust cycle and iron inputs to the ocean. *Glob. Biogeochem. Cycles* 19. <https://doi.org/10.1029/2004GB002402>.

Marcotte, A.R., Anbar, A.D., Majestic, B.J., and Herckes, P. (2020). Mineral dust and iron solubility: Effects of composition, particle size, and surface area. *Atmosphere (Basel)* 11. <https://doi.org/10.3390/atmos11050533>.

Markaki, Z., Loÿe-Pilot, M.D., Violaki, K., Benyahya, L., and Mihalopoulos, N. (2010). Variability of atmospheric deposition of dissolved nitrogen and phosphorus in the Mediterranean and possible link to the anomalous seawater N/P ratio. *Mar. Chem.* 120, 187–194. <https://doi.org/10.1016/j.marchem.2008.10.005>.

Martiny, A.C., Lomas, M.W., Fu, W., Boyd, P.W., Chen, Y. ling L., Cutter, G.A., Ellwood, M.J., Furuya, K., Hashihama, F., Kanda, J., et al. (2019). Biogeochemical controls of surface ocean phosphate. *Sci. Adv.* 5, eaax0341. <https://doi.org/10.1126/sciadv.aax0341>.

Mather, R.L., Reynolds, S.E., Wolff, G.A., Williams, R.G., Torres-Valdes, S., Woodward, E.M.S., Landolfi, A., Pan, X., Sanders, R., and Achterberg, E.P. (2008). Phosphorus cycling in the North and South Atlantic Ocean subtropical gyres. *Nat. Geosci.* 1, 439–443. <https://doi.org/10.1038/ngeo232>.

Mélançon, J., Levasseur, M., Lizotte, M., Scarratt, M., Tremblay, J.E., Tortell, P., Yang, G.P., Shi, G.Y., Gao, H., Semeniuk, D., et al. (2016). Impact of ocean acidification on phytoplankton assemblage, growth, and DMS production following Fe-dust additions in the NE Pacific high-nutrient, low-chlorophyll waters. *Biogeosciences* 13, 1677–1692. <https://doi.org/10.5194/bg-13-1677-2016>.

Meskhidze, N., Chameides, W.L., and Nenes, A. (2005). Dust and pollution: A recipe for enhanced ocean fertilization? *J. Geophys. Res. D Atmos.* 110, 1–23. <https://doi.org/10.1029/2004JD00508>.

Mills, M.M., Ridame, C., Davey, M., La Roche, J., and Geider, R.J. (2004). Iron and phosphorus co-limit nitrogen fixation in the eastern tropical North Atlantic. *Nature* 429, 292–294. <https://doi.org/10.1038/nature02550>.

Moore, C.M., Mills, M.M., Achterberg, E.P., Geider, R.J., LaRoche, J., Lucas, M.I., McDonagh, E.L., Pan, X., Poulton, A.J., Rijkenberg, M.J.A., et al. (2009). Large-scale distribution of Atlantic nitrogen fixation controlled by iron availability. *Nat. Geosci.* 2, 867–871. <https://doi.org/10.1038/ngeo667>.

Moore, C.M., Mills, M.M., Langlois, R., Milne, A., Achterberg, E.P., La Roche, J., and Geider, R.J. (2008). Relative influence of nitrogen and phosphorus availability on phytoplankton physiology and productivity in the oligotrophic sub-tropical North Atlantic Ocean. *Limnol. Oceanogr.* 53, 291–305. <https://doi.org/10.4319/lo.2008.53.1.0291>.

Murphy, J., and Riley, J.P. (1962). A modified single solution method for the determination of phosphate in natural waters. *Anal. Chim. Acta* 27, 31–36.

Okin, G.S., Mahowald, N., Chadwick, O.A., and Artaxo, P. (2004). Impact of desert dust on the biogeochemistry of phosphorus in terrestrial ecosystems. *Glob. Biogeochem. Cycles* 18. <https://doi.org/10.1029/2003GB002145>.

Orchard, E.D., Ammerman, J.W., Lomas, M.W., and Dyrhman, S.T. (2010a). Dissolved inorganic and organic phosphorus uptake in *Trichodesmium* and the microbial community: The importance of phosphorus ester in the Sargasso Sea. *Limnol. Oceanogr.* 55, 1390–1399. <https://doi.org/10.4319/lo.2010.55.3.1390>.

Orchard, E.D., Benitez-Nelson, C.R., Pellechia, P.J., Lomas, M.W., and Dyrhman, S.T. (2010b). Polyphosphate in *Trichodesmium* from the low-phosphorus Sargasso Sea. *Limnol. Oceanogr.* 55, 2161–2169. <https://doi.org/10.4319/lo.2010.55.5.2161>.

Orchard, E.D., Webb, E.A., and Dyrhman, S.T. (2009). Molecular analysis of the phosphorus starvation response in *Trichodesmium* spp. *Environ. Microbiol.* 11, 2400–2411. <https://doi.org/10.1111/j.1462-2920.2009.01968.x>.

Paytan, A., Mackey, K.R.M., Chen, Y., Lima, I.D., Doney, S.C., Mahowald, N., Labiosa, R., and Post, A.F. (2009). Toxicity of atmospheric aerosols on marine phytoplankton. *Proc. Natl. Acad. Sci. U. S. A.* 106, 4601–4605. <https://doi.org/10.1073/pnas.0811486106>.

Polyviou, D., Hitchcock, A., Baylay, A.J., Moore, C.M., and Bibby, T.S. (2015). Phosphite utilization

by the globally important marine diazotroph *Trichodesmium*. *Environ. Microbiol. Rep.* 7, 824–830. <https://doi.org/10.1111/1758-2229.12308>.

Pulido-Villena, E., Rrolle, V., and Guieu, C. (2010). Transient fertilizing effect of dust in P-deficient LNLC surface ocean. *Geophys. Res. Lett.* 37. <https://doi.org/10.1029/2009GL041415>.

Ramos, A.G., Martel, A., Codd, G.A., Soler, E., Coca, J., Redondo, A., Morrison, L.F., Metcalf, J.S., Ojeda, A., Suárez, S., and Petit, M. (2005). Bloom of the marine diazotrophic cyanobacterium *Trichodesmium erythraeum* in the Northwest African Upwelling. *Mar. Ecol. Prog. Ser.* 301, 303–305.

Rivero-Calle, S., Del Castillo, C.E., Gnanadesikan, A., Dezfouli, A., Zaitchik, B., and Johns, D.G. (2016). Interdecadal *Trichodesmium* variability in cold North Atlantic waters. *Glob. Biogeochem. Cycles* 30, 1620–1638. <https://doi.org/10.1002/2015GB005361>.

Rubin, M., Berman-Frank, I., and Shaked, Y. (2011). Dust-and mineral-iron utilization by the marine dinitrogen-fixer *Trichodesmium*. *Nat. Geosci.* 4, 529–534. <https://doi.org/10.1038/ngeo1181>.

Rueter, J.G., Hutchins, D.A., Smith, R.W., and Unsworth, N.L. (1992). Iron nutrition in *Trichodesmium*. In *Marine Pelagic Cyanobacteria: Trichodesmium and Other Diazotrophs*, E.J. Carpenter, D.G. Capone, and J.G. Rueter, eds. (Kluwer Academic), pp. 289–306.

Sañudo-Wilhelmy, S.A., Kustka, A.B., Gobler, C.J., Hutchins, D.A., Yang, M., Lwiza, K., Burns, J., Capone, D.G., Raven, J.A., and Carpenter, E.J. (2001). Phosphorus limitation of nitrogen fixation by *Trichodesmium* in the central Atlantic Ocean. *Nature* 411, 66–69. <https://doi.org/10.1038/35075041>.

Sañudo-Wilhelmy, S.A., Tovar-Sanchez, A., Fu, F.X., Capone, D.G., Carpenter, E.J., and Hutchins, D.A. (2004). The impact of surface-adsorbed phosphorus on phytoplankton Redfield stoichiometry. *Nature* 432, 897–901. <https://doi.org/10.1038/nature03125>.

Sarthou, G., Baker, A.R., Blain, S., Achterberg, E.P., Boye, M., Bowie, A.R., Croot, P., Laan, P., De Baar, H.J.W., Jickells, T.D., and Worsfold, P.J. (2003). Atmospheric iron deposition and sea-surface dissolved iron concentrations in the eastern Atlantic Ocean. *Deep. Res. Part I* 50, 1339–1352. [https://doi.org/10.1016/S0967-0637\(03\)00126-2](https://doi.org/10.1016/S0967-0637(03)00126-2).

Shoenfelt, E.M., Winckler, G., Lamy, F., Anderson, R.F., and Bostick, B.C. (2018). Highly bioavailable dust-borne iron delivered to the Southern Ocean during glacial periods. *Proc. Natl. Acad. Sci. U. S. A.* 115, 11180–11185. <https://doi.org/10.1073/pnas.1809755115>.

Sohm, J.A., Mahaffey, C., and Capone, D.G. (2008). Assessment of relative phosphorus limitation of *Trichodesmium* spp. in the North Pacific, North Atlantic, and the North coast of Australia. *Limnol. Oceanogr.* 53, 2495–2502. <https://doi.org/10.4319/lo.2008.53.6.2495>.

Stihl, A., Sommer, U., and Post, A.F. (2001). Alkaline phosphatase activities among populations of the colony-forming diazotrophic

cyanobacterium *Trichodesmium* spp. (cyanobacteria) in the red sea. *J. Phycol.* 37, 310–317. <https://doi.org/10.1046/j.1529-8817.2001.037002310.x>.

Stockdale, A., Krom, M.D., Mortimer, R.J.G., Benning, L.G., Carlsaw, K.S., Herbert, R.J., Shi, Z., Myriokefalitakis, S., Kanakidou, M., and Nenes, A. (2016). Understanding the nature of atmospheric acid processing of mineral dusts in supplying bioavailable phosphorus to the oceans. *Proc. Natl. Acad. Sci. U. S. A.* 113, 14639–14644. <https://doi.org/10.1073/pnas.1608136113>.

Sunda, W.G., and Huntsman, S.A. (1995). Iron uptake and growth limitation in oceanic and coastal phytoplankton. *Mar. Chem.* 50, 189–206. [https://doi.org/10.1016/0304-4203\(95\)00035-P](https://doi.org/10.1016/0304-4203(95)00035-P).

Tang, W., Cerdán-García, E., Berthelot, H., Polyviou, D., Wang, S., Baylay, A., Whitby, H., Planquette, H., Mowlem, M., Robidart, J., and Cassar, N. (2020). New insights into the distributions of nitrogen fixation and diazotrophs revealed by high-resolution sensing and sampling methods. *ISME J.* 14, 2514–2526. <https://doi.org/10.1038/s41396-020-0703-6>.

Thingstad, T.F., Krom, M.D., Mantoura, R.F.C., Flaten, C.A.F., Groom, S., Herut, B., Kress, N.,

Law, C.S., Pasternak, A., Pitta, P., et al. (2005). Nature of phosphorus limitation in the ultraoligotrophic eastern Mediterranean. *Science* 309, 1068–1071. <https://doi.org/10.1126/science.1112632>.

Torfstein, A., Kienast, S.S., Yarden, B., Rivlin, A., Isaacs, S., and Shaked, Y. (2020). Bulk and export production fluxes in the Gulf of Aqaba, Northern Red Sea. *ACS Earth Sp. Chem.* 4, 1461–1479. <https://doi.org/10.1021/acsearthspacechem.0c00079>.

Torfstein, A., Teutsch, N., Tirosh, O., Shaked, Y., Rivlin, T., Zipori, A., Stein, M., Lazar, B., and Erel, Y. (2017). Chemical characterization of atmospheric dust from a weekly time series in the north Red Sea between 2006 and 2010. *Geochim. Cosmochim. Acta* 211, 373–393. <https://doi.org/10.1016/j.gca.2017.06.007>.

Tyrrell, T. (1999). The relative influences of nitrogen and phosphorus on oceanic primary production. *Nature* 400, 525–531. <https://doi.org/10.1038/22941>.

Van Mooy, B.A.S., Fredricks, H.F., Pedler, B.E., Dyhrman, S.T., Karl, D.M., Koblížek, M., Lomas, M.W., Mincer, T.J., Moore, L.R., Moutin, T., et al. (2009). Phytoplankton in the ocean use non-

phosphorus lipids in response to phosphorus scarcity. *Nature* 458, 69–72. <https://doi.org/10.1038/nature07659>.

Walsby, A.E. (1992). The gas vesicles and buoyancy of *Trichodesmium*. In *Marine Pelagic Cyanobacteria: Trichodesmium and Other Diazotrophs*, E.J. Carpenter, D.G. Capone, and J.G. Rueter, eds. (Kluwer Academic), pp. 141–161. [https://doi.org/10.1007/978-94-015-7977-3\\_9](https://doi.org/10.1007/978-94-015-7977-3_9).

Wang, R., Balkanski, Y., Boucher, O., Ciais, P., Peñuelas, J., and Tao, S. (2015). Significant contribution of combustion-related emissions to the atmospheric phosphorus budget. *Nat. Geosci.* 8, 48–54. <https://doi.org/10.1038/ngeo2324>.

Wu, J., Sunda, W., Boyle, E.A., and Karl, D.M. (2000). Phosphate depletion in the western North Atlantic Ocean. *Science* 289, 759–762. <https://doi.org/10.1126/science.289.5480.759>.

Zhang, Z., Goldstein, H.L., Reynolds, R.L., Hu, Y., Wang, X., and Zhu, M. (2018). Phosphorus speciation and solubility in aeolian dust deposited in the interior American West. *Environ. Sci. Technol.* 52, 2658–2667. <https://doi.org/10.1021/acs.est.7b04729>.

## STAR★METHODS

## KEY RESOURCES TABLE

REAGENT or RESOURCE	SOURCE	IDENTIFIER
Chemicals, peptides, and recombinant proteins		
Calcium carbonate (CaCO <sub>3</sub> )	Sigma-Aldrich	Cat#481807-5G
P-coated CaCO <sub>3</sub>	This manuscript	
Potassium dihydrogen phosphate (KH <sub>2</sub> PO <sub>4</sub> )	Merck	Cat#1048731000
Ammonium molybdate ((NH <sub>4</sub> ) <sub>6</sub> Mo <sub>7</sub> O <sub>24</sub> · 4H <sub>2</sub> O)	Sigma-Aldrich	Cat#A1343-100G
L-ascorbic acid (C <sub>6</sub> H <sub>8</sub> O <sub>6</sub> )	Sigma-Aldrich	Cat#A7506-100G
Sulfuric acid (H <sub>2</sub> SO <sub>4</sub> )	Sigma-Aldrich	Cat#258105-500ML
Potassium antimony tartrate (C <sub>4</sub> H <sub>4</sub> KO <sub>7</sub> Sb)	Sigma	P-6949
RNAlater™ stabilization solution	Invitrogen	Cat#AM7021
RNeasy Mini Kit	Qiagen	Cat#74104
RNase-free DNase Kit	Qiagen	Cat#79254
Qubit RNA HS Assay kit	Invitrogen	Cat#Q32852
Qubit DNA HS Assay kit	Invitrogen	Cat#Q32851
SYBR Green I master mix	Zhishan Biotech	Cat#190417
M-MLV reverse transcriptase	BMI, Shenzhen, China	Cat#2018092001
Taq polymerase	Tiagen Biotech	Cat#ET101-02
β-mercaptoethanol	Sigma	Cat#M3148-100ML
Experimental models: Organisms/strains		
<i>Trichodesmium</i> IMS101 culture	NCMA	CCMP1985
Software and Algorithms		
IBM® SPSS® Statistics	IBM	Version (25.0)
DinoCapture 2.0	AnMo Electronics Corporation	Version: 1.5.43
Other		
Stereoscopic microscope	Nikon	SMZ745
Phytoplankton net	Aquatic Research Instrument, USA	100 μm
Real-time PCR System	Bio-Rad, Singapore	CFX96 TOUCH
Fast Prep-24™ 5G	MP Biomedicals, USA	116005500

## RESOURCE AVAILABILITY

## Lead contact

Further information and requests for resources and reagents should be directed to and will be fulfilled by the lead contact, Yeala Shaked ([yeala.shaked@mail.huji.ac.il](mailto:yeala.shaked@mail.huji.ac.il)).

## Materials availability

P-coated CaCO<sub>3</sub> generated in this study was prepared using trace-metal clean calcium carbonate powder (99.999% purity, Cat#481807-5G, Sigma-Aldrich) and KH<sub>2</sub>PO<sub>4</sub> (Cat#1048731000, Merck). Preparation procedure and P-adsorption and desorption determination were described in STAR Method text as well as in supplementary materials.

## Data and code availability

- All of the raw data collected during this study are publicly available as supplementary materials as of the date of publication.

- This paper does not report original code.
- Any additional information required to reanalyze the data reported in this paper is available from the lead contact upon request.

## EXPERIMENTAL MODEL AND SUBJECT DETAILS

### *Trichodesmium* IMS101 culture

Laboratory culture of *Trichodesmium erythraeum* IMS101 was employed to examine the physical property (“stickiness”) of synthesized particles used in this study (see later “Method details” – “Particle preparation and description” – “P-free and P-rich particles” section). The culture was grown at 26°C with 10:14 h light-dark cycles at  $\sim 80 \mu\text{E m}^{-2} \text{sec}^{-1}$  in a modified YBC-II medium that contained 50  $\mu\text{M}$  Fe and 50  $\mu\text{M}$  P.

## METHOD DETAILS

### Experiment overview

During the 2019 *Trichodesmium* spp. fall bloom in the Gulf of Aqaba we conducted incubation experiments on 17 individual days, encompassing an entire bloom season, using  $\sim 1,200$  natural puff-shaped colonies. Each incubation experiment involved 20-100 freshly collected *Trichodesmium* colonies incubated with P-free  $\text{CaCO}_3$ , P-rich  $\text{CaCO}_3$ , and dust. We documented and scored colony-particle interactions under a stereoscope at three different time points, and combined these interaction scores to form a single colony interaction index that assesses the temporal aspect of colony-particle interactions. In parallel, we examined the expression of the P stress marker *sphX* in freshly collected colonies ( $T_0$ ) on 6 different days to assess the P limitation status of *Trichodesmium* colonies throughout the season.

### Colony collection

*Trichodesmium* colonies were collected from the Gulf of Aqaba in the Red Sea (29.56°N, 34.95°E). A 100  $\mu\text{m}$  phytoplankton net was repeatedly towed at 20 m depths for 7-10 min with a motorboat, at 1-2 knots. The total volume of seawater filtered in each tow ranged from 16-62  $\text{m}^3$  and colony density ranged from 0.06-3 colony/ $\text{m}^3$ . The net concentrate was quickly transferred to 10 L acid-cleaned buckets and diluted in fresh seawater to increase colony survival. Puff-shaped colonies were subsequently hand-picked from buckets using sterile plastic droppers, and washed 3x by transferring them into petri dishes with 0.2  $\mu\text{m}$ -filtered seawater (FSW) under a stereoscope. Puff-shaped colonies, which can visibly be observed to collect and center particles, were collected for our experiments in order to assess colony-particle interactions. Integral and well-shaped colonies of similar size were individually selected and placed into separate wells of a 96-well plate, containing 150  $\mu\text{l}$  FSW and allowed to acclimate for at least 15 min prior to particle addition (see below). Colonies were randomly distributed between treatments, ensuring equal distribution of different morphotypes (typically 10-40 colonies per treatment).

Several morphotypes of puff-shaped colonies were observed throughout the season. On November 17th and 19th, we separated two distinct morphotypes, “thin” and “dense”, and compared their tendency to interact with particles. Both morphotypes of colonies share a similar colony diameter ( $\approx 1$  mm), but differ in their core volume, with small (0.008  $\text{mm}^3$ ,  $n=18$ ) and large cores (0.022  $\text{mm}^3$ ,  $n=25$ ) for thin and dense colonies, respectively.

### Particle preparation and description

**P-free and P-rich particles.** To ensure a P-free control in our experiments, we purchased a high-purity, trace-metal clean calcium carbonate powder (99.999% purity). P-rich particles were generated by mixing 10  $\text{mg ml}^{-1}$   $\text{CaCO}_3$  with 50  $\mu\text{M}$   $\text{KH}_2\text{PO}_4$  in FSW and shaking it for 24 h. The P-adsorbed  $\text{CaCO}_3$  particles were subsequently collected by centrifugation, transferred into trace-metal clean glass beakers with FSW and dried at 90°C for 24 h. We repeated the same procedure with P-free  $\text{CaCO}_3$  using FSW without the addition of  $\text{KH}_2\text{PO}_4$ . No Fe-enrichment occurred during the adsorption of P onto particles since the background contamination of Fe in the  $\text{KH}_2\text{PO}_4$  solution was low and comparable to that of the seawater used for suspending particles.

We studied the efficiency of P-adsorption on  $\text{CaCO}_3$  and the kinetics of P-desorption by measuring dissolved  $\text{PO}_4^{3-}$  concentrations according to the ascorbic acid-molybdate blue method (Murphy and Riley,

1962) using a Cary 50 Varian UV-visible spectrophotometer. The adsorption of P on  $\text{CaCO}_3$  particles was confirmed by calculating the loss of  $\text{PO}_4^{3-}$  from  $\text{KH}_2\text{PO}_4$  solution and by direct measurements of total P content of the particles (following their dissolution in hydrochloric acid). Both methods showed that at least 85% of the initially added  $\text{PO}_4^{3-}$  was adsorbed by  $\text{CaCO}_3$ , to form P-rich  $\text{CaCO}_3$  (Figure S1). We followed the P desorption kinetics to ensure that the particles retain some P throughout the experiment and to estimate the P released during the incubation. These experiments showed that ~3% of the P was desorbed from P-rich  $\text{CaCO}_3$  to FSW prior to the incubation, while most of the P remained associated with  $\text{CaCO}_3$  and continued to be released with time (Figure S1). No P was detected in the P-free  $\text{CaCO}_3$ .

We confirmed that the adsorption of P onto particles did not increase their adhesion (or “stickiness”) using *Trichodesmium* IMS101 filaments, which typically do not interact with particles (Kessler et al., 2020a; Rubin et al., 2011). Indeed, IMS101 did not interact with any of these particles, indicating that selection of P-rich particles by natural colonies is not due to the particle’s stickiness.

**Dust particles.** Dust deposited on flat and clean surfaces (i.e. roof, window shades) at IUI was physically removed and collected into a vial for this study. These dust particles originated from Sahara desert, Arabian Peninsula and local sources, and they may also contain some anthropogenic aerosols from Europe (Chen et al., 2007; MacKey et al., 2012; Torfstein et al., 2017). Dust was sieved through a 63  $\mu\text{m}$  mesh to remove large particles and washed by FSW to remove toxic components prior to the incubation with natural colonies (Kessler et al., 2020a).

### Determination of colony-particle interactions

**Incubation experiments.** Freshly collected *Trichodesmium* spp. colonies were placed in a 96-well plate, incubated with P-free and P-rich  $\text{CaCO}_3$  particles, and maintained over a 24 h timeframe in a culture room at 25°C with 10:14 h light-dark cycles ( $\sim 80 \mu\text{E m}^{-2} \text{s}^{-1}$ ) using cool, fluorescent white light. Particles were added to wells of a 96-well plate, each containing one individual *Trichodesmium* spp. colony, by pipetting 15  $\mu\text{l}$  of a 10  $\text{mg ml}^{-1}$  particle-seawater suspension directly to the colony (final particle concentration of 1  $\text{mg ml}^{-1}$ ). Parallel incubations of 10-20 colonies with dust particles were conducted using the same procedure as with  $\text{CaCO}_3$  particles.

**Assessment of colony-particle interactions.** Colony-particle interactions with P-free and P-rich  $\text{CaCO}_3$  particles were observed and assessed according to three parameters as derived by Kessler et al. (2020a) for dust interactions (Kessler et al., 2020a). The scoring criteria for each parameter was slightly modified due to the weaker interactions observed between colonies and  $\text{CaCO}_3$  in comparison to dust (Kessler et al., 2020a). As exemplified in Figure 1, the three parameters include: short-term interactions (ST, tested 15 min after particle addition), centering (tested after 1.5 h), and long-term interactions (LT, tested after overnight-incubation; 13-27 h). For each parameter, the observed colony-particle interaction was assigned one of three scores based on careful observations under a stereoscope.

**Single-colony index.** To characterize the colony collection and selection behavior, a single-colony index was constructed by compiling all 27 possible variations of the three scores (3x3x3) for a single colony (Table S1). This index hereby records the dynamics of a colony-particle interaction for the duration of the incubation period, where each variation concerns a pattern that is indicative of the overall tendency of an individual colony to collect or remove particles (Figure 2). Analyzing the index of all colonies yielded 12 common patterns that described ~90% of the colonies (Table S2). The 12 patterns were further grouped into four categories showing increasing levels of colony-particle interactions (Figure 2).

### Examination of P stress in natural colonies

To assess whether natural colonies were P-limited or not during the season, we examined the expression of the P stress marker gene *sphX* of 40 *in situ* colonies on 6 individual days and 40 colonies (in duplicates) incubated in a culture room with and without the addition of 5  $\mu\text{M}$   $\text{PO}_4^{3-}$  for 24 h.

**Sampling and RNA preservation.** Natural colonies collected from each experiment were filtered onto 5  $\mu\text{m}$  GE polycarbonate filters by gravity. Filters were then immediately folded and placed into 1.8 ml RNase-free CryoTubes™ containing 1.5 ml RNA stabilization solution. Samples were frozen at  $-80^\circ\text{C}$  or ice (during the shipment) until RNA extraction at Xiamen University, China.



**RNA extraction and qRT-PCR.** The RNA stabilization solution in each sample was carefully removed and total RNA was extracted using the RNeasy Mini Kit according to manufacturer instructions, with the following modifications. Briefly, buffer RLT containing 1%  $\beta$ -mercaptoethanol and RNase-free glass beads (0.1 mm diameter) were added to samples, and the tubes were vortexed for 45 s by Fast Prep machine, placed on ice for 1 min, and vortexed again for 45 s. The homogenized lysate was processed according to Qiagen's protocol, including on column DNase digestion using RNase-free DNase Kit to remove genomic DNA. The resulting RNA was eluted in RNase-free water and subsequently quantified using the Qubit RNA HS Assay kit according to the manufacturer's protocol. The extracted RNA was converted to single-stranded cDNA by using M-MLV reverse transcriptase in a 20  $\mu$ l reaction volume containing 150 ng of random primers, 1 mM dNTP mix and 10 mM DTT. All cDNA was stored at -20 or -80°C.

**Standard preparation and qPCR analysis.** The clade-specific primers of housekeeping gene *rnpB* and *sphX* were originally described by Chappell and Webb (2010) and Dalin Shi's laboratory protocols, and were relisted in Table S3. The dominant *Trichodesmium* sp. clade in experiments was characterized using the clade-specific *rnpB* primers.

The clade-specific *rnpB* and *sphX* amplicons were amplified by PCR, separated by gel electrophoresis, purified and ligated to the pMD 18-T vector (Takara, Japan), and then cloned into DH5a *Escherichia coli* competent cells. Plasmid DNA from cultured clones were purified and sequenced to confirm specificity. The positive sequenced plasmids were quantified using the Qubit DNA HS Assay kit and were used as standards.

All qPCR reactions were performed using a fluorescent quantitative instrument CFX 96 TOUCH. A SYBR Green I master mix was used for qPCR in 20  $\mu$ l reactions containing approximately 5  $\mu$ l of diluted template cDNA, 0.4 mM dNTPs, 200 nM each of the forward and reverse primers and 0.05 U Taq polymerase. Reactions were conducted in triplicate using the following program: 95°C for 3 min, followed by 39 cycles of 95°C for 15 s, 60°C for 30 s and 72°C for 30 s. Standards ranging from 10<sup>1</sup> to 10<sup>9</sup> gene copies per well were amplified on each plate with the cDNA generated from samples. Negative controls with nuclease-free water diluting cDNA extracts were amplified on each plate to make sure contamination was not present in the reactions. The standard curve efficiencies were always between 90 and 95% with R<sup>2</sup> values > 0.99. The specificity of qPCR reactions was confirmed by melting curve analysis and sequencing analysis. The copy numbers of the target genes in each sample were calculated from the standard curve. Relative expressions of *sphX* in samples were derived by normalizing copy number of *sphX* to copy numbers of *rnpB* in the same well.

### Compilation of particle selection studies

**Experimental and technical differences.** The study of Kessler et al., 2020a was performed in spring 2016, while this study in fall 2019. This may result in significant differences in the colony's nutritional status and morphotypes. The studies differ also by the type and amount of dust used for the experiments (5 and 1,000 mg L<sup>-1</sup> for Kessler et al., 2020a and this study, respectively.). Besides, the two studies employed different scoring criteria to assess colony-particle interactions.

**Comparison.** In order to overcome the differences among studies, we combined all colonies that were assunged with positive scores + and ++). Then we plot (Figure 9) the percentage of colonies that retained particles after the overnight-incubation (LT), ) against the percentage of colonies that initially interacted with particles (ST). Dead or opened-up colonies were excluded from the analysis. This analysis totally covered 461 and 1,104 natural colonies incubated with 9 types of particles in Kessler et al. (2020a) and this study, respectively.

### QUANTIFICATION AND STATISTICAL ANALYSES

Statistical differences among P-free CaCO<sub>3</sub>, P-rich CaCO<sub>3</sub> and dust treatments were analyzed through a contingency table using IBM SPSS software (v25.0). Depending on the sample size (n represents the total number of colonies), a 2-sided Fisher's exact (n = 38 for P-free CaCO<sub>3</sub> and 36 for P-rich CaCO<sub>3</sub> treatments) or Pearson's X-squared (n = 459 for P-free CaCO<sub>3</sub>, 475 for P-rich CaCO<sub>3</sub>, and 170 for dust treatments) test was employed for determining significance between treatments (p<0.05). Cramer's V-value was simultaneously measured for assessing the association-strength between treatments.